The PTBP1-NCOA4 axis promotes ferroptosis in liver cancer cells

HAO YANG[1], WENSHENG SUN[2], TAO BI[3], QI WANG[2], WENTAO WANG[2], YOUXIN XU[1], ZHIQIAN LIU[1*] and JIE LI[1*]

[1]Department of Hepatobiliary Surgery, The First Affiliated Hospital of Shandong First Medical University, [2]Department of Hepatobiliary Surgery, Shandong Provincial Qianfoshan Hospital, Shandong University, Jinan, Shandong 250014; [3]Department of Gastrointestinal Surgery, Yantai Affiliated Hospital of Binzhou Medical University, Yantai, Shandong 264100, P.R. China

Received July 29, 2022; Accepted November 10, 2022

DOI: 10.3892/or.2023.8482

Abstract. Polypyrimidine tract-binding protein 1 (PTBP1) plays an important role in tumor immunity, cell proliferation, apoptosis, and autophagy by regulating RNA metabolism. However, the specific function and mechanism of PTBP1 in ferroptosis remain unclear. In the present study, it was investigated whether PTBP1 regulates ferroptosis and the exact mechanism. The iron, malondialdehyde (MDA), and GSH levels were detected in sorafenib (SF)-treated liver cancer cells. si-PTBP1 introduction into SF-treated liver cancer cells resulted in a significant reduction in the levels of MDA and iron. Additionally, a significant recovery of GSH levels was observed after silencing PTBP1. StarBase v2.0 database was used to predict potential transcripts that can physically interact with PTBP1 and nuclear receptor coactivator 4 (*NCOA4*) mRNA was identified as the most enriched binding partner in the PTBP1-RNA complex. A dual-luciferase assay then demonstrated that PTBP1 directly interacted with *NCOA4*. *PTBP1* silencing did not affect NCOA4 stability following treatment with cycloheximide. A pull-down assay revealed that the PTBP1-binding region was in the 5'-UTR of the *NCOA4* mRNA sequence. These results suggest that PTBP1 mediates ferroptosis in liver cancer cells by regulating NCOA4 translation. *In vivo* experiments reconfirmed the role of the PTBP1-*NCOA4* axis in a xenograft transplantation model. It was observed that the mean tumor weight increased after *PTBP1* knockout. In conclusion, silencing of PTBP1 decreased the sensitivity of liver cancer cells to ferroptosis after SF treatment and regulated ferritinophagy by mediating NCOA4 translation.

Correspondence to: Professor Jie Li or Dr Zhiqian Liu, Department of Hepatobiliary Surgery, The First Affiliated Hospital of Shandong First Medical University, 16766 Jingshi Road, Jinan, Shandong 250014, P.R. China
E-mail: heplijie@163.com
E-mail: liuzqhbp@163.com

*Contributed equally

Key words: ferritinophagy, ferroptosis, PTBP1, RNA-binding protein, NCOA4

Introduction

Approximately 19 million new cancer cases were reported globally in 2020, with hepatocellular carcinoma (HCC) patients accounting for ~900,000. The number of deaths due to liver cancer annually is ~83,000, which is second only to that due to lung cancer (1). In recent years, targeted therapy has rapidly developed. Sorafenib (SF), known as the first-line drug for patients with advanced HCC, has been corroborated as not only a multikinase inhibitor but also a ferroptosis inducer (2,3). However, the underlying mechanism of SF-induced ferroptosis remains elusive.

Ferroptosis is a form of programmed cell death mainly characterized by iron and lipid peroxide accumulation (4). Ferroptosis occurs widely in various human diseases, such as Parkinson's disease (5), cardiovascular diseases (6), and cancer (7). Ferroptosis is not an independent process and is associated with endoplasmic reticulum (ER) stress, autophagy, and apoptosis. Ferroptosis plays a common role in regulated cell death and is induced by the selective inhibition of the cystine/glutamate transporter system x_C^- (8). In addition, ferritinophagy, the autophagic degradation of ferritin that leads to ferroptosis, is mediated by nuclear receptor coactivator 4 (NCOA4) (9). p53, a tumor suppressor, plays an important role in apoptosis. Accumulating evidence has demonstrated that p53 regulates metabolism and indirectly regulates ferroptosis (10).

Polypyrimidine tract-binding protein 1 (PTBP1) shuttles between the nucleus and cytoplasm and has a molecular weight of 58 kDa (11). PTBP1 is not only involved in the regulation of mRNA splicing and translation but also participates in mRNA transport and metabolism (12). PTBP1 has diverse functions in numerous biological processes. In the nervous system, PTBP1 is involved in regulating neuron development and growth (13). PTBP1 also mediates immune regulation. PTBP1 is involved in $CD4^+$ cell activation (14), the alternative splicing of CD46 (15), and the production of antibodies to B-cell receptors (16). PTBP1 plays an important role in cholesterol synthesis and glycolysis. PTBP1 regulates cholesterol synthesis through the

low-density lipoprotein receptor (LDLR). PTBP1 is involved in the process of glycolysis by upregulating PKM2 (17).

However, the specific function and mechanism of PTBP1 in ferroptosis remain unclear. Therefore, it was investigated whether PTBP1 could regulate ferroptosis in SF-treated liver cancer cells and investigated its molecular mechanism and function.

Materials and methods

Culture of cell lines and transfection. Cellcook Biotech Company provided 4 cell lines used in the study, including Huh-7 (cat. no. CC0102), Hep3B (cat. no. CC0103), HepG2 (cat. no. CC0118), and 293T (cat. no. CC4003). The Huh-7, HepG2 and Hep3B cell lines used in the present study were authenticated by STR profiling. All cells were cultured in DMEM or MEM, (Gibco; Thermo Fisher Scientific, Inc.) in an incubator at 37˚C under 5% CO_2. Additionally, 10% fetal bovine serum and 1% penicillin-streptomycin solution (both from Gibco; ThermoFisher Scientific, Inc.) were added to the medium. Small-interfering RNAs (siRNAs) targeting *PTBP1* and the NCOA4-overexpression plasmid (pcDNA 3.1; NM_001145262.2) were obtained from Shanghai GenePharma Co., Ltd. Huh-7 and HepG2 cells ($5x10^5$) seeded in six-well plates were transfected with si-PTBP1 or si-NC (75 pmol/well) and oe-NCOA4 or pcDNA 3.1 (5 μg/well), and Lipofectamine™ 2000 reagent (7.5 μl/well) was used to enhance the transfection according to the manufacturer's instructions. The sequences of these siRNAs or shRNAs are provided in Table SI. Short hairpin RNAs (shRNAs) against *PTBP1* were synthesized by Shanghai Genechem Co., Ltd. Overexpression or knockdown was confirmed by western blot analysis (WB) or reverse transcription-quantitative polymerase chain reaction (RT-qPCR) analyses. Cells were treated with 5 μM SF or dimethyl sulfoxide (DMSO) for 24 h before use in the subsequent experiments.

RNA extraction and RT-qPCR. The cell and tissue samples were lysed, and the total RNA was extracted with TRIzol reagent (Invitrogen; Thermo Fisher Scientific, Inc.). After genomic DNA extraction, Hiscript RT superMix was used to obtain cDNA according to the manufacturer's instructions. Two-step RT-qPCR (Vazyme Biotech Co., Ltd.) was performed on a real-time fluorescence quantitative PCR system (CFX96; BioRad Laboratories, Inc.) according to the manufacturer's instructions for ChamQ Universal SYBR qPCR Master Mix (Vazyme Biotech Co., Ltd.). The qPCR amplification protocol was as follows: 95˚C for 30 sec and followed by 40 cycles at 95˚C for 10 sec; and 60˚C for 30 sec. The $2^{-\Delta\Delta Cq}$ method was used to quantify the relative expression levels, with GAPDH selected as the reference gene (18). The primer sequences (5'-3') are listed in Table SII.

WB. Radioimmunoprecipitation lysis buffer (Beyotime Institute of Biotechnology) was used to extract proteins from the tissues and cells. The BCA assay method was performed to determine protein concentration. The proteins were fully denatured for 5 min. A total of 10 μl protein per lane was loaded for gel electrophoresis and 10% sodium dodecyl sulfate polyacrylamide gel electrophoresis was used for protein separation. Next, the proteins were transferred onto polyvinylidene difluoride (PVDF) membranes (MilliporeSigma) and the membranes were blocked with 5% fat-free milk at room temperature for 2 h. The membranes were then incubated overnight at 4˚C with primary antibodies, washed three times, and then incubated with goat anti-rabbit IgG HRP-conjugated secondary antibodies (cat. no. E-AB-1003; 1:5,000 dilution; Elabscience Biotechnology, Inc.) for 1 h at room temperature. The following antibodies were used: anti-PTBP1 (cat. no. 72669; 1:1,000; Cell Signaling Technology, Inc.), anti-ferritin heavy chain 1 (FTH1; cat. no. ab75973; 1:1,000; Abcam), anti-NCOA4 (cat. no. 66849; 1:1,000; Cell Signaling Technology, Inc.), anti-GAPDH (cat. no. 5174; 1:1,000; Cell Signaling Technology, Inc.), and anti-glutathione peroxidase 4 (cat. no. ab231174; GPX4; 1:1,000; Abcam). The membranes were detected by chemiluminescence (MilliporeSigma). ImageJ software (version 1.53; National Institutes of Health) was used for densitometric analysis.

Cell Counting Kit-8 (CCK-8) and bioinformatics analyses. Cell survival of Huh-7 and HepG2 was detected with Cell Counting Kit-8 (cat. no. E-CK-A362; Elabscience Biotechnology, Inc.) according to the manufacturer's instructions. Cells ($5x10^3$) were seeded into 96-well plates and treated with SF or DMSO for 24 h. A total of 10 μl of CCK-8 reagent was added to each well and incubation followed for 3 h at 37˚C in a 5% CO_2 incubator. The OD value at 450 nm was measured using a microplate spectrophotometer (BioTek Instruments, Inc.) and the cell survival rate was calculated.

The 33 candidate genes were selected to explore the specific mechanism of PTBP1 in ferroptosis using the Kyoto Encyclopedia of Genes and Genomes (KEGG) database (https://www.kegg.jp). In addition, RBPmap (http://rbpmap.technion.ac.il; version 1.2) was used to identify a potential binding region of PTBP1.

C11-BODIPY 581/591 fluorescent probe staining. According to the instructions, C11-BODIPY 581/591 (cat. no. RM02821; ABclonal Biotech Co., Ltd.) was diluted at 1:200, added to a Petri dish, and incubated at 37˚C for 1 h. Huh-7 or HepG2 cells were then incubated with 4% paraformaldehyde (Wuhan Servicebio Technology, Co., Ltd.) for 10 min in the dark. The fluorescence intensity of the sample was observed under a confocal microscope (Nikon A1+; Nikon Corporation).

Lipid peroxidation assay. Lipid peroxidation was evaluated with a lipid peroxidation [malondialdehyde (MDA)] assay kit (cat. no. ab118970; Abcam) according to the manufacturer's instructions. After the Huh-7 and HepG2 cells were completely lysed with MDA lysis buffer, the supernatant was extracted by centrifugation for 10 min, and a part of the sample was stored for protein quantification. Subsequently, 600 μl thiobarbituric acid (TBA) solution was added to the samples, and the samples were incubated at 95˚C for 60 min. Finally, 200 μl of each sample were added to a 96-well plate. The experiment was performed three times. After measuring the absorbance of the sample, the MDA concentration was calculated based on the standard curve.

Glutathione assay. The treated Huh-7 and HepG2 cells were detected with a glutathione (GSH) detection kit (cat. no. A006-2-1); Nanjing Jiancheng Bioengineering Institute)

according to the manufacturer's instructions, mixed well, and incubated for 5 min at room temperature. The absorbance was measured at 405 nm. Moreover, the protein concentration in the samples was determined according to the standard curve determined by a BCA assay. The GSH content was calculated based on the standard curve.

Intracellular iron. An iron assay kit (cat. no. ab83366; Abcam) was used to test the intracellular iron levels according to the manufacturer's instructions. Following the addition of 200 μl of iron assay buffer, the samples were incubated for 10 min at room temperature to completely lyse the Huh-7 and HepG2 cells. An ultrasonic cell wall-breaking apparatus (JY-IIN; Ningbo Scientz Biotechnology Co., Ltd.) was used to lyse the cells, which were then centrifuged at 12,000 x g for 10 min at 4˚C, and 150 μl of the supernatant were collected. After adding 100 μl of iron probe, the sample was incubated at room temperature for 1 h, and the absorbance was measured at 593 nm.

RNA immunoprecipitation (RIP) assay. The RIP assay was performed using an EZ-Magna RIP kit (cat. no. 17-700; MilliporeSigma) according to the manufacturer's instructions. Huh-7 cells were lysed on ice for 5 min. Immunoprecipitation was performed by adding 100 μl of magnetic beads protein A/G and 5 μg of anti-PTBP1 (cat. no. 32-4800; Thermo Fisher Scientific, Inc.), and the samples were incubated at room temperature for 30 min. The samples were added to the immunoprecipitated magnetic bead complex, incubated overnight at 4˚C, treated with protease K buffer, and incubated at 55˚C for 30 min for protein digestion, and 400 μl of phenol, chloroform, and isoamyl alcohol solution were added for RNA purification. The obtained RNA was sequenced by RT-qPCR, and the DNA amplified by qPCR was analyzed by agarose gel electrophoresis. Additionally, 1% agarose gels were selected for electrophoresis and ethidium bromide (1 μg/ml) solution was applied for staining of the agarose gel for 20 min at room temperature.

Dual-luciferase reporter assay. Psi-check2 luciferase vector (Promega Corporation) with or without NCOA4 and pcDNA3.1 or oe-PTBP1 were co-transfected into 293T cells with the aid of Lipofectamine™ 2000 reagent. The cells were collected 48 h post-transfection to detect luciferase activity. After the cells were lysed, 100 μl Stop & Glo® Reagent (Promega Corporation) were added to the samples. The *Renilla* luciferase and firefly luciferase values were determined by dual-luciferase reporter system (part no. E1910; Promega Corporation) and the method of comparison with firefly luciferase activity was adopted to normalize luciferase activity.

Pull-down assay. The constructed biotin-labeled NCOA4 mRNA 5'-untranslated region (UTR) fragment and the negative control fragment were obtained from Viagene Biotechnology Biotech, Inc. The probe sequence for the NCOA4 mRNA pulldown was as follows: Biotin-5'-GGU UAUGCUUUUAAUGGAAGCAGAUACAAAAU; negative control sequence Biotin-5'-CGATATAGAGACGAT TGGCTGGGCCCCTG. Huh-7 cells were lysed using IP lysis buffer (cat. no. 87787; Thermo Fisher Scientific, Inc.) and centrifuged at 12,000 x g for 10 min at 4˚C. The 100-μl lysates were subsequently added to the biotinylated probe and co-incubated at room temperature for at least 30 min. The complexes were isolated using prepared strepavidin-coupled Dynabeads according to the manufacturer's instructions (cat. no. 11205D; Thermo Fisher Scientific, Inc.). Following the addition of 1X protein sample loading buffer, the samples were incubated at 95˚C for 10 min and the products were analyzed using WB with antibodies against PTBP1 (cat. no. 72669; 1:1,000; Cell Signaling Technology, Inc.).

Cycloheximide (CHX) chase assay. To evaluate whether PTBP1 influenced the stability of NCOA4, Huh-7 cells were transfected with PTBP1 siRNAs, incubated for 24 h, treated with 20 μg/μl CHX (Sigma-Aldrich; Merck KGaA) for the indicated time-points (0, 15, 30, 60 and 120 min) to inhibit protein synthesis, and subjected to WB.

Nascent protein analysis. A new protein synthesized analysis was performed using Click-iT AHA for Nascent Protein Synthesis (cat. no. C10102; Invitrogen; Thermo Fisher Scientific, Inc.) and Click-iT Biotin protein analysis detection kits (cat. no. C33372; Invitrogen; Thermo Fisher Scientific, Inc.) according to the manufacturer's instructions. Methionine-free medium was added to the cells to deplete methionine reserves and AHA for 4 h. After Huh-7 cells lysed, the samples were prepared for the Click-iT® detection reaction. Nascent proteins were pulled down and analyzed by WB.

Mouse xenograft model. A total of eight male BALB/c nude mice (4-5 weeks old; weight, 13-18 g) were obtained from Beijing Vital River Laboratories. The mice were raised in specific pathogen-free conditions with food and water *ad libitum*, and the rearing environment was maintained with a 12-h light/dark cycle at a temperature of 26-28˚C and a relative humidity of 50±10%. All animal experiments were approved by the Animal Care and Use Committee of Shandong Provincial Qianfoshan Hospital (approval no. S725). The mice were randomly divided into the following two groups: The NC + SF and sh-PTBP1 + SF groups. Hep3B cells ($2x10^6$) were subcutaneously injected into the right flank of each mouse. The mice were injected intraperitoneally with SF (10 mg/kg) every 2 days for 2 weeks. The mice were sacrificed by CO_2 euthanasia four weeks later, and the tumors were harvested. The tumor volume was calculated as follows: V=0.5 (length x width^2). A portion of the hepatic tumor tissue was extracted to measure the iron, MDA, and GSH levels.

Statistical analyses. The statistical analyses were performed using GraphPad 8 software (GraphPad Software, Inc.). The data are presented as line charts or bar charts. The differences between two independent samples were compared using an independent-samples t-test. All experiments were repeated three times. $P<0.05$ was considered to indicate a statistically significant difference.

Results

Silencing of PTBP1 positively regulates the sensitivity of liver cancer cells to ferroptosis. For a preliminary verification of whether PTBP1 was associated with ferroptosis in liver cancer,

Huh-7 and HepG2 cells were treated with SF (5 μM) for 24 h. RT-qPCR and WB were performed to observe the relative expression of PTBP1. PTBP1 was significantly increased in the SF groups compared with the blank and DMSO groups in the HepG2 and Huh-7 cell lines (Fig. 1A and B). These results suggest that PTBP1 is a key factor in SF-induced ferroptosis. The CCK-8 results revealed that liver cancer cells viability significantly decreased under SF induction. Compared with the NC + SF group, the cell viability was higher in the si-PTBP1 group, suggesting that the sensitivity to ferroptosis decreased after silencing of PTBP1 (Fig. 1C and D). Next, the iron, MDA, and GSH levels were detected. The MDA and iron levels were significantly reduced in the si-PTBP1+ SF group compared with those in the NC + SF group (Fig. 1E and F). Additionally, cells transfected with si-PTBP1 showed an increase in intracellular GSH levels after SF treated for 24 h (Fig. 1G). The liquid peroxide levels were observed using C11 BODIPY 581/591. When C11-BODIPY is oxidized, the fluorescence signal changes from red (nonoxidized) to green (oxidized) (19). The green fluorescence signal intensity (oxidized) was significantly weakened after transfection of si-PTBP1, as observed under a confocal microscope (Fig. 1H). Correspondingly, these results indicate that decreased PTBP1 expression reduced the sensitivity to ferroptosis.

PTBP1 targets NCOA4 and regulates ferroptosis in liver cancer cells. To explore the specific mechanism of PTBP1 in ferroptosis, 33 genes in the ferroptosis pathway (map04216) were first selected using the KEGG database as candidate molecules (Table SIII). Subsequently, 14,331 downstream genes of *PTBP1* were predicted by StarBase v2.0 (http://starbase.sysu.edu.cn) (Fig. 2A). Finally, 15 key genes were identified as *PTBP1* targets (number of binding sites >20) (Fig. 2B). The downstream binding sites of PTBP1 were further verified using a RIP-qPCR assay. The fold changes of *NCOA4*, *ATG7*, *ATG5*, *ACSL4* and *PCBP2* enriched by anti-PTBP1 were significantly higher than those in the anti-IgG group (Fig. 2C). NCOA4 was finally selected as the major target because of the highest fold change among the 15 candidate genes. The RT-qPCR amplification products of *NCOA4* were subjected to nucleic acid gel electrophoresis. The results revealed that PTBP1 interacts with *NCOA4* mRNA (Fig. 2D). To verify the direct interaction between PTBP1 and *NCOA4*, a dual-luciferase assay was performed and it was revealed that PTBP1 overexpression increased luciferase activity in 293T cells transfected with psi-check2-*NCOA4* but not in those transfected with pcDNA3.1, suggesting that PTBP1 can directly interact with *NCOA4* (Fig. 2E).

PTBP1 regulates the translation of NCOA4 by targeting the NCOA4 mRNA 5'-UTR. The relative *NCOA4* mRNA levels in Huh-7 cells showed no significant change after *PTBP1* silencing (Fig. 3A), whereas NCOA4 protein expression was significantly reduced (Fig. 3B). NCOA4 stability remained unaffected after the cells were treated with CHX (20 μg/μl) (Fig. 3C). Nascent protein of NCOA4 was detected, and it was observed that NCOA4 was significantly decreased after the *PTBP1* knockdown (Fig. 3D). To identify a potential binding region of PTBP1, the sites matching PBTP1 were predicted with an RBPmap. The results showed that two binding sites strongly matched to the 5'-UTR (Fig. 3E). Biotinylated segments of the 5'-UTR of *NCOA4* mRNA were then synthesized to perform pull-down assays, and the products were analyzed using WB. It was observed that PTBP1 expression was markedly enhanced in the *NCOA4* 5'-UTR group in Huh-7 cells (Fig. 3F). These results indicate that the PTBP1-binding region was in the 5'-UTR of the *NCOA4* mRNA sequence and that PTBP1 promotes NCOA4 translation by interacting with the *NCOA4* mRNA 5'-UTR. To explore the specific role of PTBP1 in the ferroptosis pathway, WB was performed. GPX4 and FTH1 expression increased after transfecting si-PTBP1 into SF-induced liver cancer cells (Fig. 3G). GPX4 converts potentially toxic lipid hydroperoxides (L-OOH) to nontoxic lipid alcohols (L-OH), while GPX4 inhibition causes the accumulation of lipid hydroperoxides, increasing ferroptosis sensitivity (4).

NCOA4 overexpression increases sensitivity to SF-induced ferroptosis. A previous study revealed that NCOA4 is a key ferroptosis regulator that promotes iron accumulation in cells (20). To verify whether PTBP1 regulates SF-induced ferroptosis by mediating NCOA4 translation, rescue experiments were performed. The levels of iron, MDA, and GSH in liver cancer cells were detected. The levels of iron and MDA were significantly reduced following si-PTBP1 transfection. The *NCOA4* overexpression successfully reversed the decreased intracellular levels of iron and MDA in liver cancer cells (Fig. 4A and B). In addition, it was observed that the increased levels of GSH following transfection with si-PTBP1 were decreased after the overexpression of NCOA4 (Fig. 4C). Collectively, the findings indicated that *NCOA4* may be a key downstream target of PTBP1 in ferroptosis regulation. Under SF-induced conditions, PTBP1 promoted NCOA4 translation, accelerated FTH1 degradation, prompted a rapid increase in the intracellular iron levels, and stimulated intracellular reactive oxygen species (ROS) accumulation.

PTBP1 promotes sensitivity to ferroptosis in vivo. To explore whether PTBP1 regulates ferroptosis in xenograft models, four-week-old mice were randomly allocated into NC + SF and sh-PTBP1 + SF groups (Fig. 5A). The tumor volumes were recorded every 3-4 days, and the mice were observed for four weeks. The tumor volumes were significantly reduced in the NC + SF group (Fig. 5B), whereas the mean tumor weight was increased in the sh-PTBP1 + SF group (Fig. 5C). Next, the relative levels of MDA, GSH, and iron were detected. The levels of MDA and iron in the tumors were significantly decreased after the knockout of PTBP1. The GSH depletion was rescued compared with that in the NC + SF group (Fig. 5D). Moreover, proteins were extracted from randomly selected tumor specimens to perform WB. The expression of FTH1 and GPX4 was increased in Hep3B cells transfected with sh-PTBP1 (Fig. 5E). These results suggest that PTBP1 promotes SF-induced ferroptosis and reveal the biological role of PTBP1 in ferroptosis progression *in vivo*.

Discussion

Previous studies have reported that ferroptosis plays a key role in SF resistance and combination therapy. Increased MT-1G expression was revealed to reduce intracellular GSH depletion,

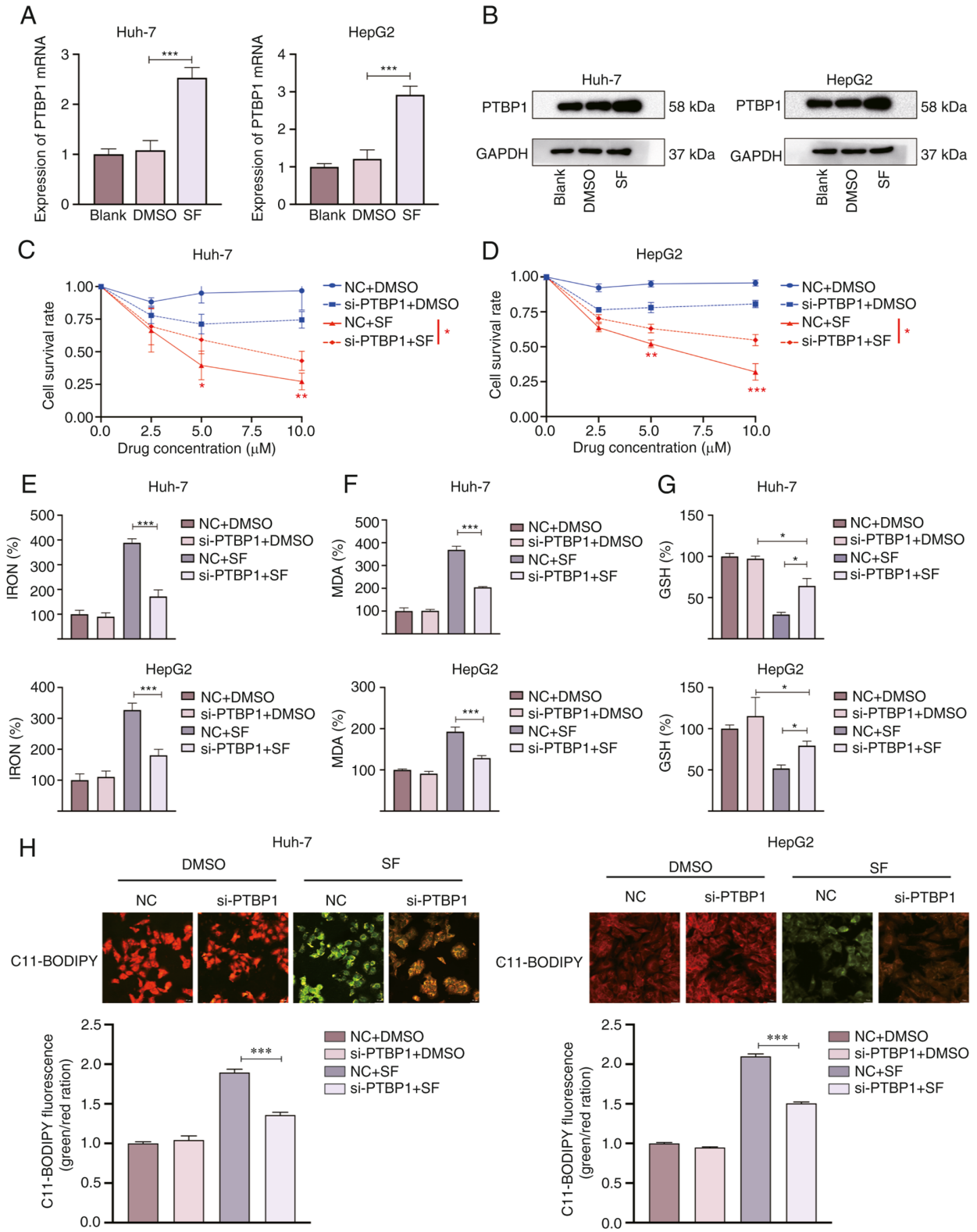

Figure 1. PTBP1 knockdown decreases the sensitivity of SF-treated liver cancer cells to ferroptosis. PTBP1 (A) mRNA and (B) protein level changes following SF treatment (5 μM, 24 h). (C and D) SF inhibited the growth of liver cancer cells as revealed by the results of the CCK-8 assay. (E-G) Changes in the levels of ferroptosis indicators in liver cancer cells after SF treatment. Following silencing of *PTBP1*, the levels of (E) iron and (F) MDA significantly decreased, whereas that of (G) intracellular GSH significantly increased. (H) Representative confocal microscopic images of C11-BODIPY 581/591 staining in SF-treated liver cancer cells. *P<0.05, **P<0.01 and ***P<0.001 (Student's t-test). PTBP1, polypyrimidine tract-binding protein 1; SF, sorafenib; CCK-8, Cell Counting Kit-8; MDA, malondialdehyde; GSH, glutathione; NC, negative control; si-, small interfering RNA.

inhibits ferroptosis, and promote SF resistance (21). GSTZ1 deletion activated the NRF2 pathway and increased GPX4 expression, thus suppressing SF-induced ferroptosis (22). YAP/TAZ was revealed to depend on TEAD to upregulate SLC7A11 expression and synergistically induce SLC7A11 expression by maintaining the stability of the ATF4 protein.

A

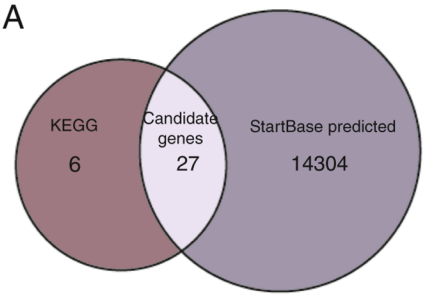

B

RBP	GeneName	ClipExpNum	Number of binding sites	PancancerNum
PTBP1	ATG7	4	145	15
PTBP1	SLC7A11	4	117	12
PTBP1	TFRC	4	86	22
PTBP1	ATG5	4	76	24
PTBP1	ACSL4	4	71	17
PTBP1	PCBP2	4	63	20
PTBP1	SLC39A8	4	44	10
PTBP1	SLC3A2	4	38	20
PTBP1	SLC11A2	4	37	17
PTBP1	STEAP3	3	33	13
PTBP1	SLC39A14	2	32	15
PTBP1	SPEG	3	29	18
PTBP1	NCOA4	4	29	19
PTBP1	LPCAT3	3	24	21
PTBP1	GCLC	4	23	12

C

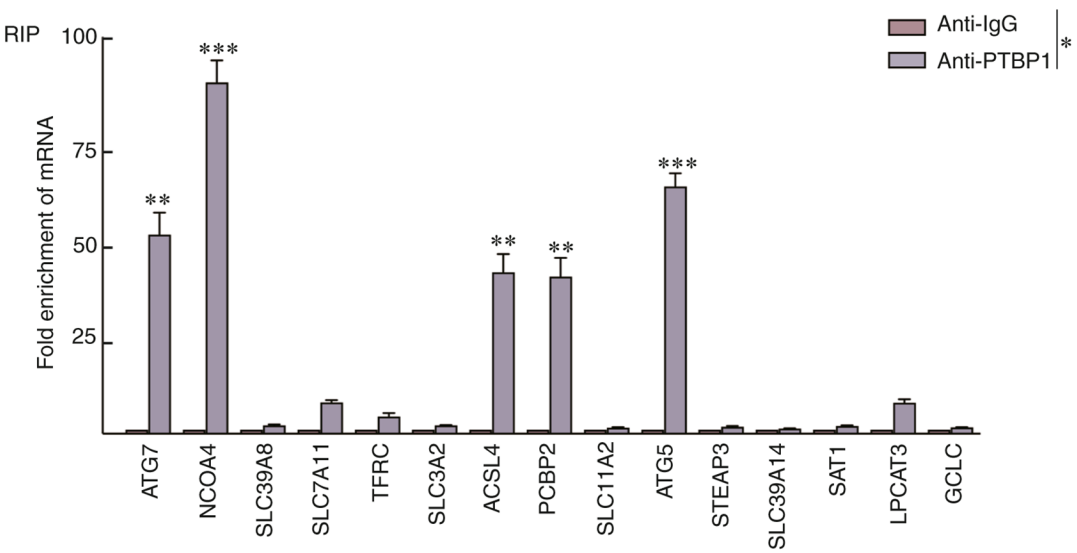

D

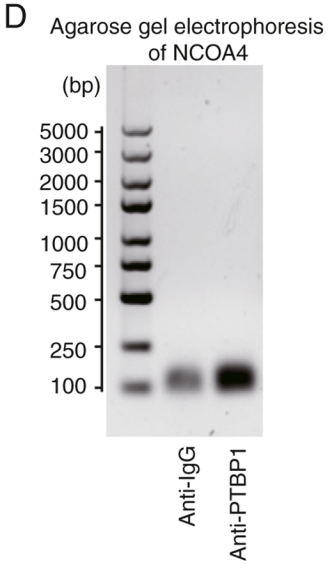

E

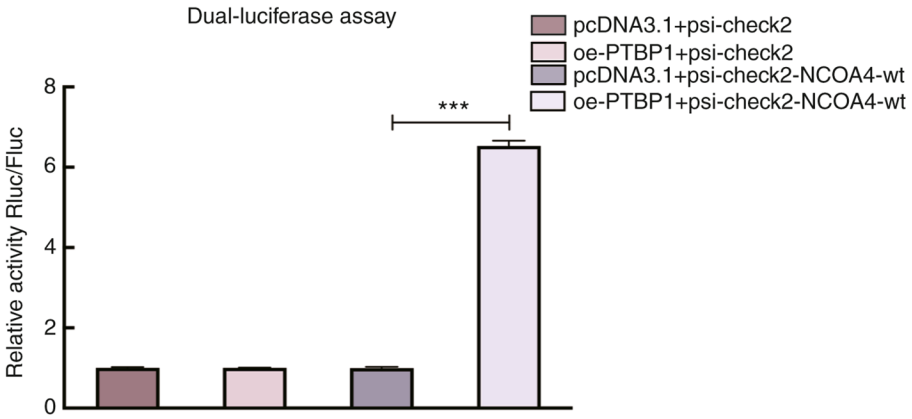

Figure 2. PTBP1 interacts with *NCOA4* to enhance ferroptosis sensitivity. (A) Intersection between key genes involved in the ferroptosis pathway in the KEGG database and the candidate genes downstream of *PTBP1* as predicted by StarBase v2.0. (B) A total of 15 candidate genes were identified, that satisfied the filtering criteria (number of binding sites >20). (C) The results of the RIP assay revealed the enrichment-fold of 15 candidate genes in PTBP1-RNA binding complexes in Huh-7 cells, with anti-IgG as the negative control. (D) Gel electrophoresis results revealed that the expression of the *NCOA4*-amplified product in the anti-PTBP1 group was significantly higher than that in the anti-IgG group. (E) Dual-luciferase reporter assay results demonstrated that the co-transfection with overexpressed PTBP1 significantly enhanced the luciferase activity of *NCOA4* in 293T cells. *P<0.05, **P<0.01 and ***P<0.001 (Student's t-test). PTBP1, polypyrimidine tract-binding protein 1; *NCOA4*, nuclear receptor coactivator 4; KEGG, Kyoto Encyclopedia of Genes and Genomes; RIP, RNA immunoprecipitation; oe-, overexpression; wt, wild-type.

High SLC7A11 expression inhibited ferroptosis and promoted SF resistance (23). Disulfiram (DSF) was demonstrated to significantly activate p62 phosphorylation, resulting in the accumulation of iron and lipid peroxides in cells and induction of ferroptosis. DSF enhanced the cytotoxicity of SF via ferroptosis and inhibited the growth of HCC cells (24). In the present study, it was demonstrated that SF upregulated the expression of PTBP1 in liver cancer cells. Compared with the control group, it was determined that the levels of iron and MDA were decreased after silencing of PTBP1. PTBP1

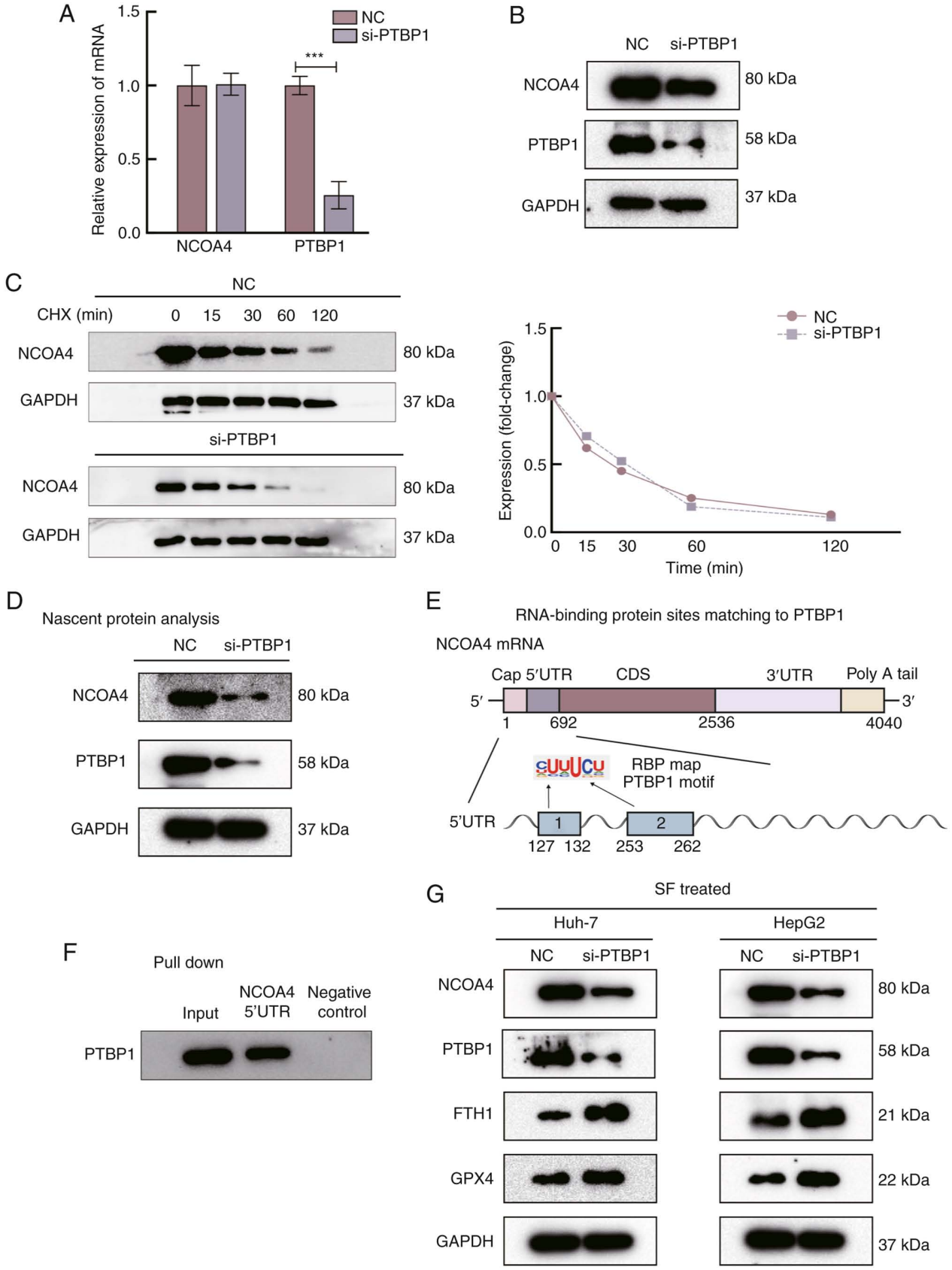

Figure 3. PTBP1 promotes ferroptosis by regulating the translation of *NCOA4*. (A) Silencing of PTBP1 did not significantly alter the mRNA levels of NCOA4. (B) The protein level of NCOA4 was significantly decreased after transfection with si-*PTBP1* for 48 h. (C) Evaluation of NCOA4 stability in Huh-7 cells treated with cycloheximide. (D) Nascent translation of NCOA4 in Huh-7 cells. The protein level of NCOA4 markedly decreased after silencing of *PTBP1*. (E) RNA-binding protein sites of PTBP1 were predicted by RBP mapping. (F) The results of the biotin pull-down analysis revealed the interaction between PTBP1 and the *NCAO4* mRNA 5'-UTR. Biotinylated *GAPDH* 3'-UTR was included as a negative control. (G) Function of PTBP1 in the ferroptosis pathway. Western blot analysis of the protein levels of PTBP1, NCOA4, FTH1 and GPX4, with GAPDH as a negative control. ***P<0.001 (Student's t-test). PTBP1, polypyrimidine tract-binding protein 1; *NCOA4*, nuclear receptor coactivator 4; si-, small interfering RNA; RBP, RNA-binding protein; FTH1, ferritin heavy chain 1; GPX4, glutathione peroxidase 4; NC, negative control; CHX, cycloheximide.

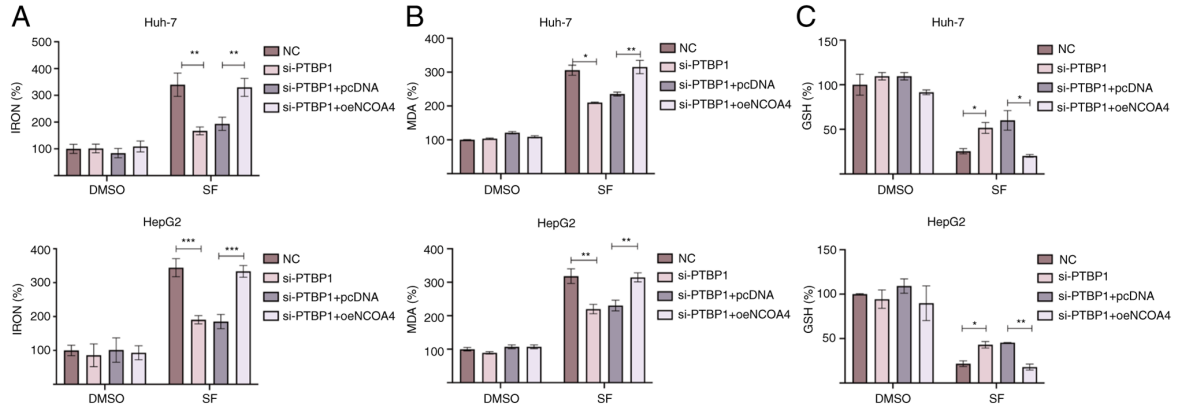

Figure 4. NCOA4 overexpression increases the sensitivity of liver cancer cells to SF-induced ferroptosis. (A) NCOA4 overexpression significantly reversed the *si-PTBP1*-mediated changes in the percentage of iron. (B) Changes in the percentage of MDA in Huh-7 and HepG2 cells treated with SF. (C) Changes in the percentage of GSH in Huh-7 and HepG2 cells treated with SF. *P<0.05, **P<0.01 and ***P<0.001 (Student's t-test). NCOA4, nuclear receptor coactivator 4; SF, sorafenib; si-, small interfering RNA; PTBP1, polypyrimidine tract-binding protein 1; MDA, malondialdehyde; GSH, glutathione; NC, negative control; oe-, overexpression.

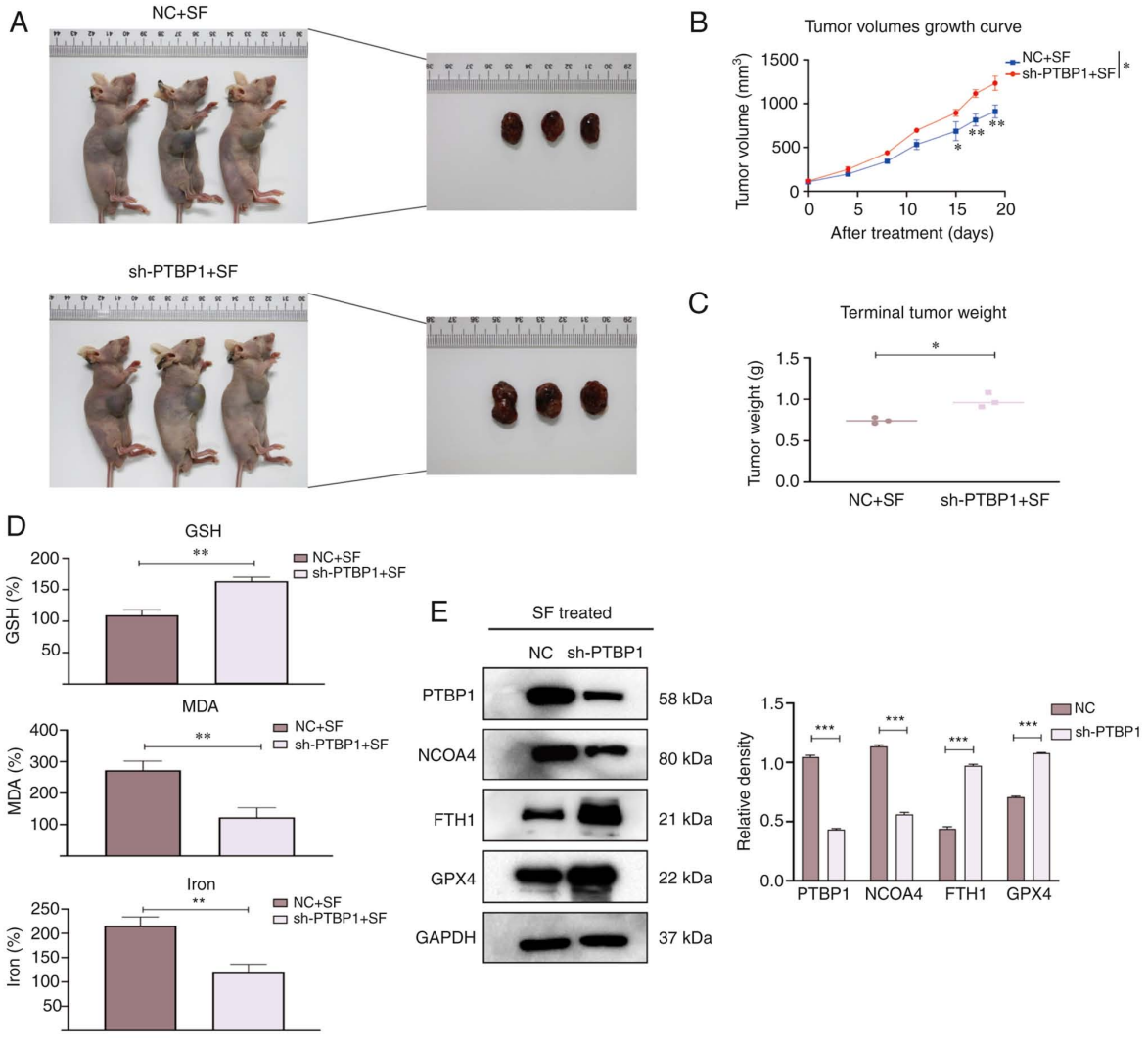

Figure 5. Biological role of PTBP1 *in vivo*. Mice were divided into two groups, namely, the NC + SF group and the sh-PTBP1 + SF group. (A) Representative images of nude mice after various treatments (mice that had succumbed and/or were deemed inelegible were excluded). (B) The tumor volume was measured every 3-4 days. An increase in the mean tumor volume was observed after silencing of *PTBP1*. (C) The mean tumor weight was decreased in the NC + SF group compared with that in the sh-PTBP1 + SF group after SF treatment for two weeks. (D) The relative levels of ferroptosis indicators, including GSH, MDA, and iron. (E) Proteins were extracted from random mouse specimens, and the levels of PTBP1, FTH1, GPX4 and NCOA4 were assessed by a western blot analysis, with GAPDH as the internal reference. *P<0.05, **P<0.01 and ***P<0.001 (Student's t-test). PTBP1, polypyrimidine tract-binding protein 1; NC, negative control; SF, sorafenib; sh-, short hairpin RNA; GSH, glutathione; MDA, malondialdehyde; FTH1, ferritin heavy chain 1; GPX4, glutathione peroxidase 4; NCOA4, nuclear receptor coactivator 4.

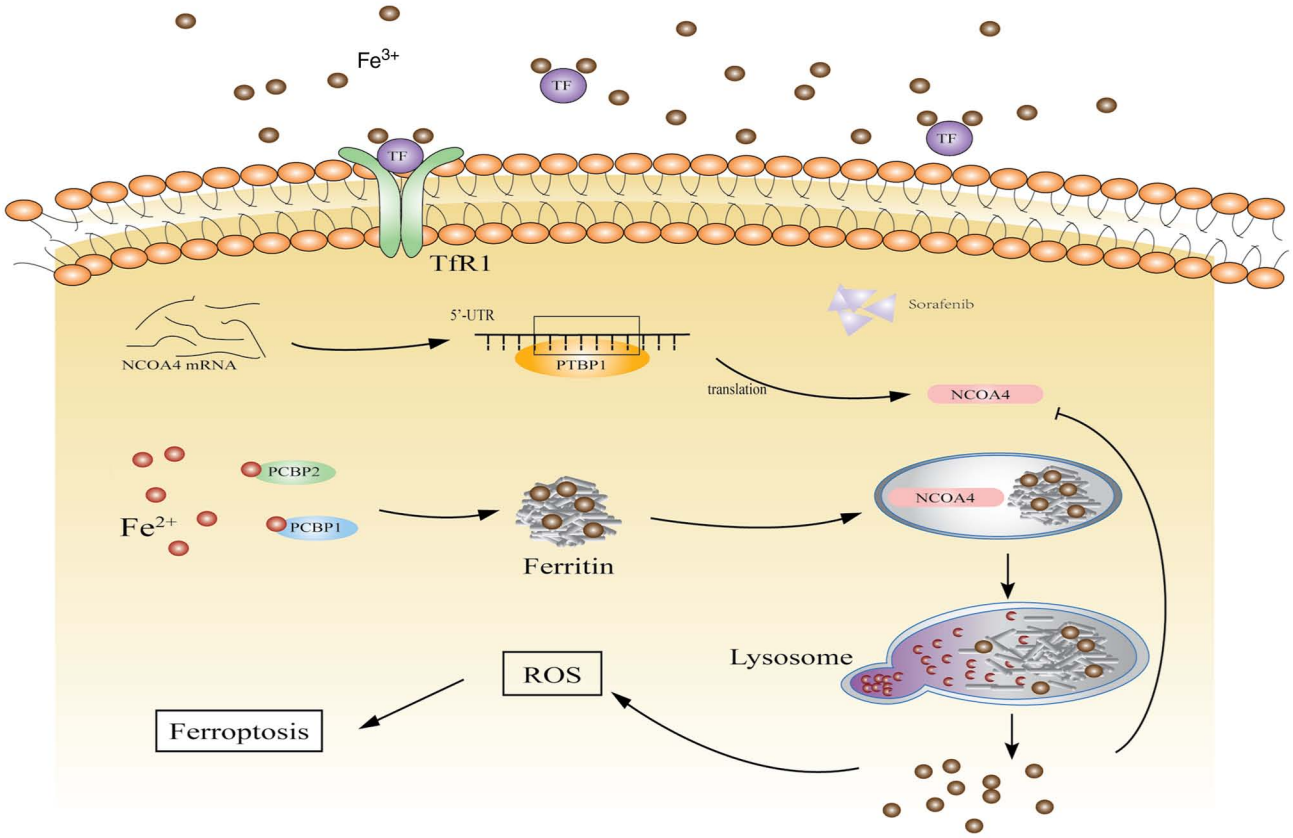

Figure 6. Schematic of the proposed mechanism of action of PTBP1 in ferroptosis in liver cancer cells. PTBP1, polypyrimidine tract-binding protein 1; NCOA4, nuclear receptor coactivator 4: ROS, reacitve oxygen species.

enhanced the sensitivity of liver cancer cells to ferroptosis and helped solve the issue of SF resistance.

RBPs are active in ferroptosis. In colorectal cancer, SFRS9 enhanced its expression by binding *GPX4* mRNA and inhibited SF and erastin-induced ferroptosis (25). hnRNPA1 induced cancer-associated fibroblasts to secrete miR-522 exosomes, resulting in ALOX15 inhibition and ROS accumulation in cancer cells and ultimately reducing ferroptosis sensitivity (26). ZFP36 inhibited *TAG6L1* mRNA stability and activated ferritinophagy to regulate ferroptosis sensitivity in hepatic stellate cells (27).

PTBP1, an RNA-binding protein, also plays an important role in ferroptosis in liver cancer cells. A previous study reported that PTBP1 was involved in autophagy regulation. The binding of lncRNA ZNF649-AS1 to PTBP1 enhanced the stability of ATG5 mRNA and promoted autophagy in breast cancer cells (28). Hou *et al* reported that silencing ATG5 and ATG7 significantly decreased the level of intracellular iron and weakened the sensitivity to ferroptosis (29). In the present study, it was further hypothesized that PTBP1 regulates ferroptosis through ferritinophagy. The results in the present study indicated an interaction between PTBP1 and *NCOA4* mRNA through RIP and dual-luciferase gene reporter assays. It was confirmed that PTBP1 regulates ferroptosis by interacting with NCOA4.

In 1996, NCOA4 was first discovered, and its 614-amino acid sequence was detected for the first time. The calculated molecular weight was 70 kDa (30). The two transcript isoforms of NCOA4 in humans are NCOA4α and NCOA4β, both of which have an N-terminal coiled-coil domain. NCOA4β only has a partial C-terminal domain, which also leads to some functional differences (31).

Research has reported that the binding sites of NCOA4 and FTH1 are located in the NCOA4α C-terminal domain but not in NCOA4β (32). Initially, NCOA4 was considered a steroid receptor coactivator widely distributed in humans (30). As research progressed, NCOA4 was identified as a cargo receptor that targets ferritin to autophagosomes during selective autophagy (33). The process of selective autophagy involves specific receptor proteins that target selected cargoes for autophagic degradation. As a selective autophagy receptor protein, NCOA4 plays an important role in ferroptosis.

Ferritinophagy plays a key role in ferroptosis. Ferritinophagy mainly mediates ferritin degradation and enhances ferroptosis sensitivity (29,34). PTBP1 promotes 'ferritinophagy' by upregulating NCOA4 expression. In the present study the interaction between PTBP1 and the *NCOA4* mRNA 5'-UTR was confirmed by a pulldown assay using biotin-labeled RNA fragments. The eukaryotic 5'-UTR plays an important role in controlling translation efficiency (35). The qPCR results showed that the *NCOA4* mRNA levels were unchanged after *PTBP1* silencing. However, NCOA4 protein expression was significantly reduced. It was inferred that PBTP1 is involved in the positive regulation of NCOA4 translation and contributes to the sensitivity of liver cancer cells to ferroptosis. NCOA4 binds ferritin via its C-terminal domain and interacts with LC3B to deliver selective cargo to autophagosomes (36). Ferritinophagy mainly recruits ferritin for degradation in the lysosome and the release of free iron.

When iron accumulates in cells, ROS are generated via the Fenton reaction, which can lead to ferroptosis (37). As a feedback mechanism, the NCOA4 expression level is closely related to the cytoplasmic iron levels (33). In previous research it was revealed that when the intracellular iron level was high, NCOA4 was degraded via the HERC2-mediated proteasomal degradation pathway (32).

In the present study, the effect of PTBP1 on ferroptosis was verified in liver cancer cells. However, whether PTBP1 plays the same role under the stimulation of ferroptosis inducers, such as RSL3 and erastin, remains to be determined. Further investigation is required. In addition, whether PTBP1 is involved in regulating ferroptosis by mediating other genes in the ferroptosis pathway remains unclear.

Overall, ferroptosis provides a new direction for tumor treatment. In the present study, the interaction between PTBP1 and NCOA4 significantly promoted the activation of ferritinophagy, enhanced the degradation of ferritin, and accelerated the accumulation of intracellular iron (Fig. 6). The findings of the present study revealed the function of PTBP1 in ferroptosis. Furthermore, studying the specific mechanism of SF in liver cancer may aid in solving the issue of SF resistance.

Acknowledgements

Not applicable.

Funding

The present study was supported by the National Natural Science Foundation of China (grant nos. 82172830 and 82002504), and the Shandong Provincial Key Research and Development Program (grant no. 2019GSF108053).

Availability of data and materials

The datasets used during the present study are available from the corresponding author upon reasonable request.

Authors' contributions

HY performed the experiments, and contributed to data curation, formal analysis and writing of the original draft, as well as review and editing of the manuscript. JL and ZL contributed to design of the study, funding acquisition and writing, review and editing. WS and TB contributed to western blotting and writing of the original draft. QW, WW and YX contributed to cell culture and interpreted some of the data. JL and ZL confirm the authenticity of all the raw data. All authors read and approve the final manuscript.

Ethics approval and consent to participate

All animal experiments were approved (approval no. S725) by the Animal Care and Use Committee of Shandong Provincial Qianfoshan Hospital (Jinan, China).

Patient consent for publication

Not applicable.

Competing interests

The authors declare that they have no competing interests.

References

1. Sung H, Ferlay J, Siegel RL, Laversanne M, Soerjomataram I, Jemal A and Bray F: Global cancer statistics 2020: GLOBOCAN estimates of incidence and mortality worldwide for 36 cancers in 185 countries. CA Cancer J Clin 71: 209-249, 2021.
2. Forner A, Reig M and Bruix J: Hepatocellular carcinoma. Lancet 391: 1301-1314, 2018.
3. Lachaier E, Louandre C, Godin C, Saidak Z, Baert M, Diouf M, Chauffert B and Galmiche A: Sorafenib induces ferroptosis in human cancer cell lines originating from different solid tumors. Anticancer Res 34: 6417-6422, 2014.
4. Stockwell BR, Friedmann Angeli JP, Bayir H, Bush AI, Conrad M, Dixon SJ, Fulda S, Gascón S, Hatzios SK, Kagan VE, *et al*: Ferroptosis: A regulated cell death nexus linking metabolism, redox biology, and disease. Cell 171: 273-285, 2017.
5. Mahoney-Sanchez L, Bouchaoui H, Ayton S, Devos D, Duce JA and Devedjian JC: Ferroptosis and its potential role in the physiopathology of Parkinson's Disease. Prog Neurobiol 196: 101890, 2021.
6. Hong M, Rong J, Tao X and Xu Y: The emerging role of ferroptosis in cardiovascular diseases. Front Pharmacol 13: 822083, 2022.
7. Liang C, Zhang X, Yang M and Dong X: Recent progress in ferroptosis inducers for cancer therapy. Adv Mater 31: e1904197, 2019.
8. Dixon SJ, Patel DN, Welsch M, Skouta R, Lee ED, Hayano M, Thomas AG, Gleason CE, Tatonetti NP, Slusher BS and Stockwell BR: Pharmacological inhibition of cystine-glutamate exchange induces endoplasmic reticulum stress and ferroptosis. Elife 3: e02523, 2014.
9. Santana-Codina N and Mancias JD: The role of NCOA4-mediated ferritinophagy in health and disease. Pharmaceuticals (Basel) 11: 114, 2018.
10. Liu Y and Gu W: p53 in ferroptosis regulation: The new weapon for the old guardian. Cell Death Differ 29: 895-910, 2022.
11. Zhu W, Zhou BL, Rong LJ, Ye L, Xu HJ, Zhou Y, Yan XJ, Liu WD, Zhu B, Wang L, *et al*: Roles of PTBP1 in alternative splicing, glycolysis, and oncogensis. J Zhejiang Univ Sci B 21: 122-136, 2020.
12. Han W, Wang L, Yin B and Peng X: Characterization of a novel posttranslational modification in polypyrimidine tract-binding proteins by SUMO1. BMB Rep 47: 233-238, 2014.
13. Vuong JK, Lin CH, Zhang M, Chen L, Black DL and Zheng S: PTBP1 and PTBP2 serve both specific and redundant functions in neuronal pre-mRNA splicing. Cell Rep 17: 2766-2775, 2016.
14. La Porta J, Matus-Nicodemos R, Valentin-Acevedo A and Covey LR: The RNA-binding protein, polypyrimidine tract-binding protein 1 (PTBP1) is a key regulator of CD4 T cell activation. PLoS One 11: e0158708, 2016.
15. Tang SJ, Luo S, Ho JXJ, Ly PT, Goh E and Roca X: Characterization of the regulation of CD46 RNA alternative splicing. J Biol Chem 291: 14311-14323, 2016.
16. Monzón-Casanova E, Screen M, Díaz-Muñoz MD, Coulson RMR, Bell SE, Lamers G, Solimena M, Smith CWJ and Turner M: The RNA-binding protein PTBP1 is necessary for B cell selection in germinal centers. Nat Immunol 19: 267-278, 2018.
17. Shan S, Shi J, Yang P, Jia B, Wu H, Zhang X and Li Z: Apigenin restrains colon cancer cell proliferation via targeted blocking of pyruvate kinase M2-dependent glycolysis. J Agric Food Chem 65: 8136-8144, 2017.
18. Livak KJ and Schmittgen TD: Analysis of relative gene expression data using real-time quantitative PCR and the 2(-Delta Delta C(T)) method. Methods 25: 402-408, 2001.
19. Carlsen CU, Kurtmann L, Bruggemann DA, Hoff S, Risbo J and Skibsted LH: Investigation of oxidation in freeze-dried membranes using the fluorescent probe C11-BODIPY(581/591). Cryobiology 58: 262-267, 2009.
20. Liu MZ, Kong N, Zhang GY, Xu Q, Xu Y, Ke P and Liu C: The critical role of ferritinophagy in human disease. Front Pharmacol 13: 933732, 2022.
21. Sun X, Niu X, Chen R, He W, Chen D, Kang R and Tang D: Metallothionein-1G facilitates sorafenib resistance through inhibition of ferroptosis. Hepatology 64: 488-500, 2016.

22. Wang Q, Bin C, Xue Q, Gao Q, Huang A, Wang K and Tang N: GSTZ1 sensitizes hepatocellular carcinoma cells to sorafenib-induced ferroptosis via inhibition of NRF2/GPX4 axis. Cell Death Dis 12: 426, 2021.
23. Gao R, Kalathur RKR, Coto-Llerena M, Ercan C, Buechel D, Shuang S, Piscuoglio S, Dill MT, Camargo FD, Christofori G and Tang F: YAP/TAZ and ATF4 drive resistance to Sorafenib in hepatocellular carcinoma by preventing ferroptosis. EMBO Mol Med 13: e14351, 2021.
24. Ren X, Li Y, Zhou Y, Hu W, Yang C, Jing Q, Zhou C, Wang X, Hu J, Wang L, *et al*: Overcoming the compensatory elevation of NRF2 renders hepatocellular carcinoma cells more vulnerable to disulfiram/copper-induced ferroptosis. Redox Biol 46: 102122, 2021.
25. Wang R, Xing R, Su Q, Yin H, Wu D, Lv C and Yan Z: Knockdown of SFRS9 inhibits progression of colorectal cancer through triggering ferroptosis mediated by GPX4 reduction. Front Oncol 11: 683589, 2021.
26. Zhang H, Deng T, Liu R, Ning T, Yang H, Liu D, Zhang Q, Lin D, Ge S, Bai M, *et al*: CAF secreted miR-522 suppresses ferroptosis and promotes acquired chemo-resistance in gastric cancer. Mol Cancer 19: 43, 2020.
27. Zhang Z, Guo M, Li Y, Shen M, Kong D, Shao J, Ding H, Tan S, Chen A, Zhang F and Zheng S: RNA-binding protein ZFP36/TTP protects against ferroptosis by regulating autophagy signaling pathway in hepatic stellate cells. Autophagy 16: 1482-1505, 2020.
28. Han M, Qian X, Cao H, Wang F, Li X, Han N, Yang X, Yang Y, Dou D, Hu J, *et al*: lncRNA ZNF649-AS1 induces trastuzumab resistance by promoting ATG5 expression and autophagy. Mol Ther 28: 2488-2502, 2020.
29. Hou W, Xie Y, Song X, Sun X, Lotze MT, Zeh HJ III, Kang R and Tang D: Autophagy promotes ferroptosis by degradation of ferritin. Autophagy 12: 1425-1428, 2016.
30. Yeh S and Chang C: Cloning and characterization of a specific coactivator, ARA70, for the androgen receptor in human prostate cells. Proc Natl Acad Sci USA 93: 5517-5521, 1996.
31. Alen P, Claessens F, Schoenmakers E, Swinnen JV, Verhoeven G, Rombauts W and Peeters B: Interaction of the putative androgen receptor-specific coactivator ARA70/ELE1alpha with multiple steroid receptors and identification of an internally deleted ELE1beta isoform. Mol Endocrinol 13: 117-128, 1999.
32. Mancias JD, Pontano Vaites L, Nissim S, Biancur DE, Kim AJ, Wang X, Liu Y, Goessling W, Kimmelman AC and Harper JW: Ferritinophagy via NCOA4 is required for erythropoiesis and is regulated by iron dependent HERC2-mediated proteolysis. Elife 4: e10308, 2015.
33. Mancias JD, Wang X, Gygi SP, Harper JW and Kimmelman AC: Quantitative proteomics identifies NCOA4 as the cargo receptor mediating ferritinophagy. Nature 509: 105-109, 2014.
34. Kang R and Tang D: Autophagy and ferroptosis-what's the connection? Curr Pathobiol Rep 5: 153-159, 2017.
35. Hinnebusch AG, Ivanov IP and Sonenberg N: Translational control by 5'-untranslated regions of eukaryotic mRNAs. Science 352: 1413-1416, 2016.
36. Goodall M and Thorburn A: Identifying specific receptors for cargo-mediated autophagy. Cell Res 24: 783-784, 2014.
37. Liu J, Kuang F, Kroemer G, Klionsky DJ, Kang R and Tang D: Autophagy-dependent ferroptosis: Machinery and regulation. Cell Chem Biol 27: 420-435, 2020.